35th Annual International Conference of the IEEE EMBS
Osaka, Japan, 3 - 7 July, 2013

# Computational Models of Optogenetic Tools for Controlling Neural Circuits with Light

Konstantin Nikolic[1], Sarah Jarvis[2], Nir Grossman[3] and Simon Schultz[2]

*Abstract*— **Optogenetics is a new neurotechnology innovation based on the creation of light sensitivity of neurons using gene technologies and remote light activation. Optogenetics allows for the first time straightforward targeted neural stimulation with practically no interference between multiple stimulation points since either light beam can be finely confined or the expression of light sensitive ion channels and pumps can be genetically targeted. Here we present a generalised computational modeling technique for various types of optogenetic mechanisms, which was implemented in the NEURON simulation environment. It was demonstrated on the example of a two classical mechanisms for cells optical activation and silencing: channelrhodopsin-2 (ChR2) and halorhodopsin (NpHR). We theoretically investigate the dynamics of the neural response of a layer 5 cortical pyramidal neuron (L5) to four different types of illuminations: 1) wide-field whole cell illumination 2) wide-field apical dendritic illumination 3) focal somatic illumination and 4) focal axon initial segment (AIS) illumination. We show that whole-cell illumination of halorhodopsin most effectively hyperpolarizes the neuron and is able to silence the cell even when driving input is present. However, when channelrhodopsin-2 and halorhodopsin are concurrently active, the relative location of each illumination determines whether the response is modulated with a balance towards depolarization. The methodology developed in this study will be significant to interpret and design optogenetic experiments and in the field of neuroengineering in general.**

## I. INTRODUCTION

Optogenetics is a technique for exciting or silencing cells within living tissue via genetic photosensitization and remote optical activation [1], [2]. This photostimulation technology allows the interrogation of neural circuits with high spatial and temporal resolution [3]. Even a single cell can be targeted at a number of very localised stimulation points [4]. In addition, it offers substantial prospects for the development of novel neuroprosthetic interfaces [5]. The photosensitization of cells is achieved by transfecting cells with an opsin, such as the light-sensitive algal protein channelrhopsin-2 (ChR2) [6], or with a light-gated chloride pump halorhodopsin NpHR [7], etc. Spatial selectivity can be achieved by genetically targeted expression of opsins, or by focusing the light beam onto targeted areas. E.g. light can be focused on a single soma using laser-coupled optical fibers or onto a large number of subcellular compartments using micro-LED arrays.

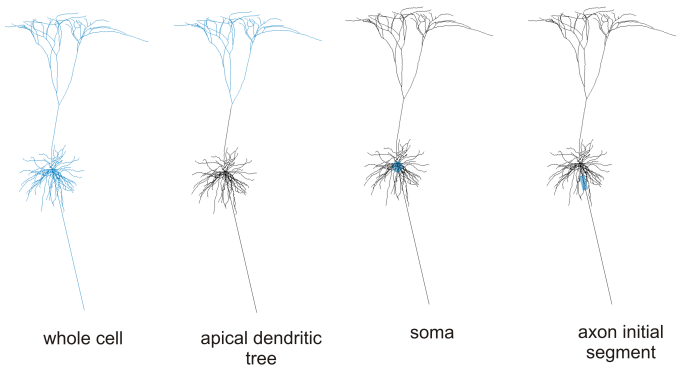


Fig. 1. Illustration of the four patterns of simulated optogenetic illuminations.

This study establishes a general methodology for modeling optogenetic channels or pumps which is based on the work on modeling ChR2 [8]–[11] (a non-selective lihgt gated ion-channel, which is an example of an excitatory mechanism), and here expanded to NpHR as an example of an inhibitory mechanism. For that purpose we used the experimental results reported in [3], [12], [13] which describe *Natronomonas pharaonis* halorhodopsin (NpHR) which is an archaeal rhodopsin functioning as an inward-directed, light driven $Cl^-$ pump. The models were devloped in the NEURON simulation environment [14] since then they can be readily incorporated into any of the neural cell models available in NeuronDB. As a model neuron here we use the pyramidal cell of layer 5b in the mammalian neocortex described in a recent study by Hay et.al [15]. The model parameters were optimised for two cases: high and low dendritic tree excitability. The photosensetized cells were optically excited with four major types of illuminations as shown in Fig. 1. We explored the impact of the illumination pattern and various combinations of excitatory and inhibitory optogenetic mechanisms on the cells spiking and the waveforms of the back-propagating action potentials (BAPs), as well the effects of simultaneous expression and activation of two opposing optogenetic modalities.

## II. MODELING OF MICROBIAL X-RHODOPSINS (XR)

### A. Functional Multi-state Models

The ionic current due to an optogenetic mechanisms XR can be expressed in the form:

$$I_{\mathrm{XR}} = A \cdot \bar{g}_{\mathrm{XR}} \cdot \psi(\phi, t) \cdot f(v) \ , \qquad (1)$$

*This work was supported by Wellcome Trust UK, grant RSRO_P41619: "Optogenetic manipulation of injured neural circuits" and grant EU FP7-ICT-2009-249867 "SeeBetter".

[1]K. Nikolic is with Institute of Biomedical Engineering, Department of Electrical and Electronic Engineering, Imperial College London, London SW7 2AZ, UK. k.nikolic@imperial.ac.uk

[2]S. Jarvis and S. Schultz are with the Department of Bioengineering, Imperial College London, London SW7 2AZ, UK. {s.jarvis,s.schultz}@imperial.ac.uk

[3]N. Grossman is with Synthetic Neurobiology Group, Depts. of Biological Engineering and Brain and Cognitive Sciences Massachusetts Institute of Technology, Cambridge, MA 02139, USA. nirg@media.mit.edu

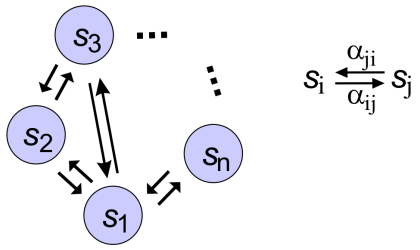


Fig. 2. Illustration of the $n$-state functional model of an optogenetic ion-channel or pump mechanism (left) and reversible transition rates between two states (right).

where $A$ is area of the cell or a compartment, $\bar{g}_{\mathrm{XR}}$ is the maximal conductance of the XR ion channels or pumps per unit area, and (normalised) functions $\psi$ and $f$ describe how the current depends on the photon flux ($\phi(t)$) and the membrane voltage $v$, respectively. The parameter $\bar{g}_{\mathrm{XR}}$ accounts for both the maximal conductance of a single XR ion channel and the protein expression (concentration) in the cell membrane. Function $f(v)$ will typically take form: $f(v) = v - E_{\mathrm{rev}}$, where $E_{\mathrm{rev}}$ is the reversal potential for the ionic species relevant for the ion channels and pumps, except for ChR2 which is better described as an inward rectifier with a function: $f(v) = (v/v_1) \cdot (1 - \exp(-v/v_0))$ [16].

The channel conductance dependence on the light intensity and internal kinetics of the molecular complex ($\psi(\phi, t)$) can be described by introducing functional states of the complex. The functional states are related to different spectroscopically identified states (e.g. see [17]), but they identify only the states relevant for the functional behaviour of the channel, hence names such as open and closed state [9]. Generally any ionic channel/pump species can be described by $n$ states: $s_1,\ s_2,\ \cdots, s_{\mathrm{n}}$, where the values for $s_{\mathrm{i}}$ are between zero and one and represent the fraction of all channels/pumps of a certain type in the state $s_{\mathrm{i}}$. The transitions between two states $s_{\mathrm{i}}$ and $s_{\mathrm{j}}$ can be described by transition rates as shown in Fig. 2: $\alpha_{\mathrm{ij}}(\phi, t) = \alpha_{\mathrm{ij,dark}} + \alpha_{\mathrm{ij,light}}(\phi(t))$, where $\alpha_{\mathrm{dark}}$ describes spontaneous, thermally driven transitions (which are always possible) and transitions induced by photon absorption $\alpha_{\mathrm{light}}(\phi(t))$. The state-space dynamics is described by a set of rate equations:

$$\frac{\mathrm{d}s_{\mathrm{i}}}{\mathrm{d}t} = -k_i s_{\mathrm{i}} + \sum_{j \neq i} \alpha_{\mathrm{ji}} s_{\mathrm{j}}\ ,\ \text{where}\ k_{\mathrm{i}} = \sum_{j \neq i} \alpha_{\mathrm{ij}} \qquad (2)$$

Note that $\sum_i s_i = 1$. Now the function $\psi$ can be defined as: $\psi(\phi) = \sum_i \gamma_{\mathrm{i}} s_{\mathrm{i}}$, where $\gamma_{\mathrm{i}}$ is the relative conductance of the state $s_{\mathrm{i}}$ in respect to the conductance of the state with the maximum conductance.

### *B. Computational Implementation for NEURON simulation platform*

The model of an ion-channel or a pump described above can be implemented in NEURON by introduction of a new mechanism of .mod type. Each mechanism can be implemented as a POINT_PROCESS module with an ELECTRODE_CURRENT. It is restricted to a small enough region so it can be described in terms of a net conductance and total current. In the localized ELECTRODE_CURRENT type point process positive currents depolarize the membrane while negative currents hyperpolarize it [14]. The pairwise n-state model scheme defined in (1) and (2) can be directly described in a KINETIC block, in which the flow between two states is defined by corresponding rate functions. The unknowns of the model scheme, i.e. the relative population of the individual states, are declared in the STATE block, which causes the NMODL translator to convert it into a family of ODEs whose variables are the states. The light dependent forward and reverse reaction rates are calculated in a separate PROCEDURE, which is called by the KINETIC block. The empirical model constant values are given in a PARAMETER block. The instantaneous flux of light is calculated in a self-events NET_RECEIVE block. The NET_RECEIVE block is essential to be used in order to define the different kinetics of the ion-channel/pump and can only be implemented in a POINT_PROCESS allowing the current to change discontinuously. The kinetic model is integrated using the sparse method that separates the Jacobian evaluation from the calculation of the STATE derivatives, which is generally faster than computing the full Jacobian matrix [14].

## III. RESULTS

For the modeling of ChR2 we use a six-state mode: two closed states (dark-adapted and light-adapted, $s_1$ and $s_6$), two open states: $s_3$ ($\gamma_3 = 1$) and $s_4$ ($\gamma = 0.05$) and two intermediate states: $s_2$ ($\gamma = 0$) and $s_5$ ($\gamma_5 = 0$). The non-zero transition rates are of the form: $\alpha_{12} = c_1(\phi(t)/\phi_0)$, $\alpha_{23} = c_2$, $\alpha_{31} = c_3$, $\alpha_{34} = c_{3d} + c_{3l}\log(\phi(t)/\phi_0)$, $\alpha_{43} = c_{4d} + c_{4l}\log(\phi(t)/\phi_0)$, $\alpha_{46} = c_4$, $\alpha_{54} = c_5$, $\alpha_{65} = c_6(\phi(t)/\phi_0)$ and $\alpha_{61} = c_7$, where the form of the rates were empirically determined, $c_i$ are constants and $\phi_0$ is a sub-threshold flux used to normalise the light flux $\phi$. Details about the choice of the states and the parameter fitting can be found in [10]. For NpHR we use a three-state model, what would be the simplest model for an ionic pump. The states are: the ground/dark-adapted closed state $s_1$ ($\gamma_1 = 0$), the open state $s_2$ ($\gamma_2 = 1$) and the desensitized state $s_3$ ($\gamma = 0$). The non-zero transition rates are: $\alpha_{12} = a_1(\phi(t)/\phi_0)$, $\alpha_{23} = a_2$ and $\alpha_{31} = a_{3d} + a_{3l}\log(\phi(t)/\phi_0)$. The parameters were chosen on the basis of the experimental results from [3] and [12].

### *A. Activation of NpHR*

We begin by examining the activation of NpHR for different illumination patterns and measuring their effect at 3 different recording sites located at the soma, proximal apical dendrite and distal apical dendrite (Fig. 3A). In the absence of any external input, activation of the NpHR pump demonstrated a clear hyperpolarization of membrane voltage at the three recording sites when the entire cell was illuminated (Fig. 3B). This was sufficient to stop the generation of action potentials created by a constant current injection of 1 nA at the soma (Fig. 3C). When the neuron was only partially illuminated in the apical dendrite, hyperpolarization of the mem-

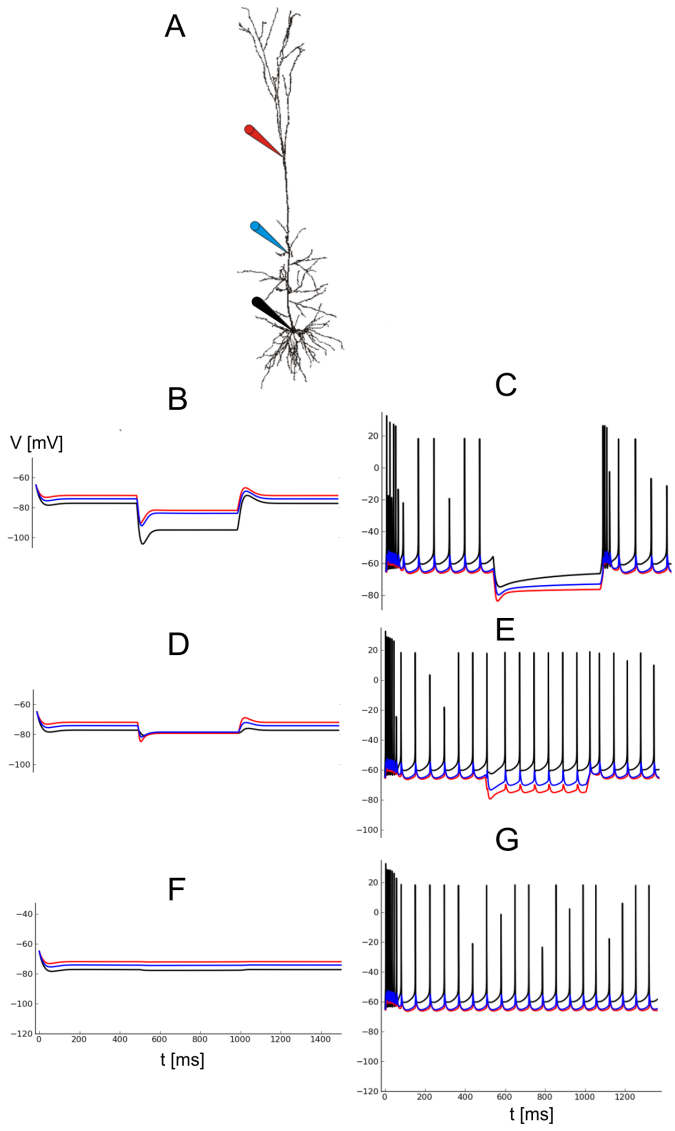


Fig. 3. Characterization of NpHR response. (A) Three recording sites, located at the soma (black), proximal apical dendrite (blue) and distal apical dendrite (red). (B) Whole-cell illumination significantly hyperpolarized the membrane. (D) Illumination at only apical dendrites produced a lesser degree hyperpolarization. (F) Illumination of the soma or axon did not significantly hyperpolarize the neuron. Current injected (1 nA) at the soma for (C) whole-cell illumination, (E) apical dendrites and (G) soma or axon. NpHR illumination from 500 to 1000ms.

brane voltage was also observed (Fig. 3D). Hyperpolarization was observable with the addition of somatic current injection but was insufficient to prevent the membrane voltage from reaching threshold (Fig. 3E). However, illumination at the soma or at the axon did not result in significant hyperpolarization of the steady state membrane voltage (Fig. 3F), and did not alter the activity of the neuron when synaptic current was injected (Fig. 3G). We note here that these findings are of qualitative nature and quantitatively valid only for the specific choice of the light intensity (10 mW/mm$^2$) and the NpHR expression, but still they demonstrate what might be expected for different stimulation protocols.

TABLE I

CO-ACTIVATION OF NPHR AND CHR2 ON FIRING RATE. LEGEND: F - NO EFFECT ON FIRING RATE (FIG. 4A); f - LOWER FIRING RATE DUE TO PARTIAL HYPERPOLARIZATION (FIG. 4B); f* - INITIAL BURST OF ACTIVITY, FOLLOWED BY STEADY-STATE HYPERPOLARIZATION AT SOMA (FIG. 4C).

| NpHR | | | | | |
|---|---|---|---|---|---|
| Whole | Apical | Soma | Axon | | |
| f | F | F | F | Whole | ChR2 |
| f* | f | F | F | Apical | |

### B. Co-activation of NpHR and ChR2

Since a detailed study about L5 cells expressing only ChR2 can be found in our recent publication [10], the effect of concurrently activating NpHR and ChR2 was then examined, for the same three recording sites as indicated in Fig. 3A. Different combinations of the four illumination patterns specified in Fig. 1 were examined, and the duration of illumination was 500ms. As illumination of ChR2 by itself at the soma and axon were not able to sufficiently depolarize the neuron and illicit action potentials for the opsin expression and illumination power values tested here, these sites were disregarded for ChR2.

We observed three different types of response: NpHR did not hyperpolarize the membrane voltage sufficiently resulting in the cell firing in a sustained manner (Fig. 4A); NpHR was able to partially hyperpolarize the membrane voltage and thus decrease the firing rate (Fig. 4B); or that the neuron was silenced after emitting a single initial burst of action potentials (Fig. 4C). The results for all illumination patterns are summarized in Table I and reveal that the fine balance that occurs with hyperpolarization and depolarization across the neuron's membrane. Whole-cell illumination for both opsins result in the generation of action potentials but at a reduced firing rate. This suggests that for equal power density and expression of opsins throughout the neuron, there is a slight imbalance towards depolarization. However, this result is dependent on the illumination values and expression of each opsin across the membrane.

While the first two responses we observed for the interaction of ChR2 and NpHR are able to be directly inferred following the results obtained from only activating NpHR (Fig. 3B-G), the last response hints at the rich interplay of subthreshold dynamics that occur locally throughout the neuron when subsections are selectively stimulated. The whole-cell illumination with NpHR and activation of ChR2 in only the apical dendrites revealed that the membrane voltage at both locations in the apical dendrite were near threshold. However, inhibition provided by NpHR acted to decouple the apical dendrite from the soma, preventing the depolarization of the membrane voltage at the soma, which after depolarizing and resulting in an initial burst of action potentials, returned to a steady-state value near the resting membrane potential.

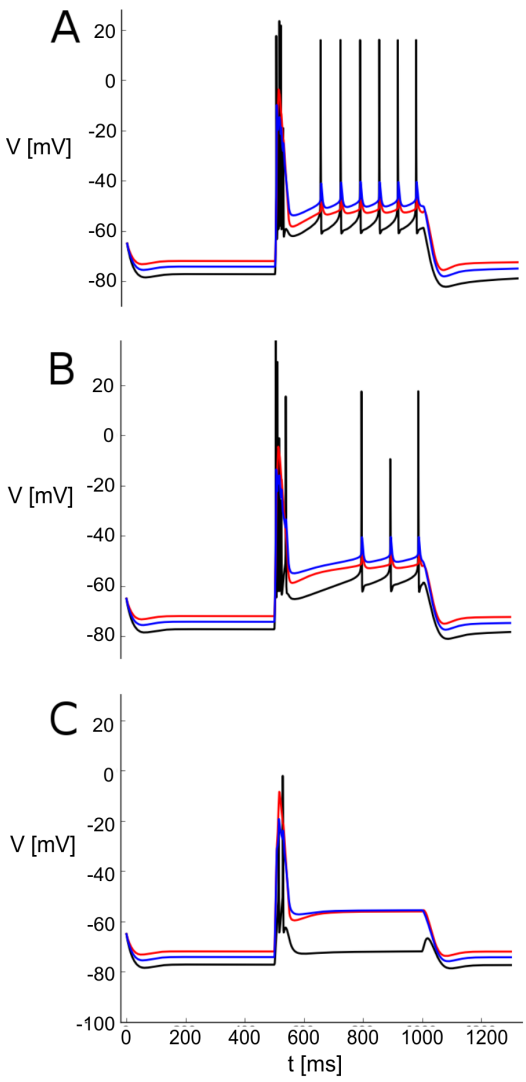


Fig. 4. Characterization of responses for concurrent activation of ChR2 and NpHR. The cell's excitation was achieved only by illuminating ChR2 without any current injection or synaptic currents, and three responses were observed when cell's silencing was attempted by activating NpHR: (A) NpHR did not sufficiently hyperpolarize the membrane, and the neuron fired due to the activaton of ChR2. (B) NpHR partially hyperpolarized the neuron, resulting in a lower firing rate. (C) After an initial burst of action potentials, hyperpolarization induced by NpHR at the soma counteracts the depolarization from ChR2 in the apical dendrites. Both illuminations occurred from 500 to 1000ms.

## IV. Discussion and Conclusions

Here was developed and demonstrated a powerful tool for computational simulations of an arbitrary optogenetic ion-channel or pump mechanism within the NEURON simulation platform. Just a small sample of possible effects are shown here on the example of two opposing mechanisms: one which acts excitatory (ChR2) and the other which acts inhibitory (NpHR). ChR2 and NpHR are compatible because they operate at similar light powers but with well-separated absorption peaks (approximately 460nm and 580 nm, respectively [7]). The two probes can be integrated on a single vector and co-expressed in mammalian brain tissue for bidirectional optical modulation of neural activity. Possibility to introduce both excitatory and inhibitory inputs into a single cell allows for control of the cell's firing at millisecond precision and offers almost complete control of neural circuits, since only having ability to elicit spikes but not to inhibit them is not enough. Many neural circuits actually have quite a wide range of excitatory inputs that converge to a neuron, but often a neuron distinguishes itself physiologically from other neurons by inhibiting the irrelevant input information.

## References


[1] E. S. Boyden, F. Zhang, E. Bamberg, G. Nagel, and K. Deisseroth, "Millisecond-timescale, genetically targeted optical control of neural activity," *Nat Neurosci*, vol. 8, no. 9, pp. 1263–8, 2005.

[2] O. Yizhar, L. E. Fenno, T. J. Davidson, M. Mogri, and K. Deisseroth, "Optogenetics in neural systems," *Neuron*, vol. 71, no. 1, pp. 9–34, 2011.

[3] F. Zhang, A. M. Aravanis, A. Adamantidis, L. de Lecea, and K. Deisseroth, "Circuit-breakers: optical technologies for probing neural signals and systems," *Nat Rev Neurosci*, vol. 8, no. 8, pp. 577–81, 2007a.

[4] N. Grossman, P. Poher, M. S. Grubb, G. T. Kennedy, K. Nikolic, B. McGovern, R. Berlinguer Palmini, Z. Gong, E. M. Drakakis, M. A. A. Neil, M. D. Dawson, J. Burrone, and P. Degenaar, "Multi-site optical excitation using chr2 and micro-led array," *Journal of Neural Engineering*, vol. 7, no. 1, p. 016004, 2010.

[5] P. Degenaar, N. Grossman, M. Memon, J. Burrone, M. Dawson, E. Drakakis, M. Neil, and K. Nikolic, "Optobionic visiona new genetically enhanced light on retinal prosthesis," *J Neural Eng*, vol. 6, no. 3, p. 035007, 2009.

[6] G. Nagel, T. Szellas, W. Huhn, S. Kateriya, N. Adeishvili, P. Berthold, D. Ollig, P. Hegemann, and E. Bamberg, "Channelrhodopsin-2, a directly light-gated cation-selective membrane channel," *Proc Natl Acad Sci U S A*, vol. 100, no. 24, pp. 13940–5, 2003.

[7] F. Zhang, L. P. Wang, M. Brauner, J. F. Liewald, K. Kay, N. Watzke, P. G. Wood, E. Bamberg, G. Nagel, A. Gottschalk, and K. Deisseroth, "Multimodal fast optical interrogation of neural circuitry," *Nature*, vol. 446, no. 7136, pp. 633–9, 2007b.

[8] P. Hegemann, S. Ehlenbeck, and D. Gradmann, "Multiple photocycles of channelrhodopsin," *Biophys J*, vol. 89, no. 6, pp. 3911–8, 2005.

[9] K. Nikolic, N. Grossman, M. S. Grubb, J. Burrone, C. Toumazou, and P. Degenaar, "Photocycles of channelrhodopsin-2," *Photochemistry and Photobiology*, vol. 85, pp. 400–411, 2009.

[10] N. Grossman, V. Simiaki, C. Martinet, C. Toumazou, S. Schultz, and K. Nikolic, "The spatial pattern of light determines the kinetics and modulates backpropagation of optogenetic action potentials," *J Comput Neurosci*, pp. DOI 10.1007/s10827–012–0431–7, 2012.

[11] S. S. Talathi, P. Carney, and P. Khargonekar, "Control of neural synchrony using channelrhodopsin-2: a computational study," *J Comput Neurosci*, vol. 31, no. 1, pp. 87–103, 2011.

[12] X. Han and E. S. Boyden, "Multiple-color optical activation, silencing, and desynchronization of neural activity, with single-spike temporal resolution," *PLoS ONE*, vol. 2, no. 3, p. e299, 2007.

[13] D. Zimmermann, A. Zhou, M. Kiesel, K. Feldbauer, U. Terpitz, W. Haase, T. Schneider-Hohendorf, E. Bamberg, and V. L. Sukhorukov, "Heterologous expression of pharaonis halorhodopsin in xenopus laevis oocytes and electrophysiological characterization of its light-driven cl2 pump activity," *Biophys J*, vol. 92, pp. 2559–69, 2007.

[14] N. Carnevale and M. Hines, "The neuron book," *Cambridge University Press*, vol. Cambridge, UK, 2006.

[15] E. Hay, S. Hill, F. Schrmann, H. Markram, and I. Segev, "Models of neocortical layer 5b pyramidal cells capturing a wide range of dendritic and perisomatic active properties," *PLoS Comput Biol*, vol. 7, no. 7, p. e1002107, 2011.

[16] N. Grossman, K. Nikolic, C. Toumazou, and P. Degenaar, "Modeling study of the light stimulation of a neuron cell with channelrhodopsin-2 mutants," *Biomedical Engineering, IEEE Transactions on*, vol. 58, no. 6, pp. 1742–1751, 2011.

[17] O. P. Ernst, P. A. Sanchez Murcia, P. Daldrop, S. P. Tsunoda, S. Kateriya, and P. Hegemann, "Photoactivation of channelrhodopsin," *J Biol Chem*, vol. 283, no. 3, pp. 1637–43, 2008.